Received: 21 June 2021 | Revised: 3 September 2021 | Accepted: 3 September 2021

DOI: 10.1111/gcb.15881

Global Change Biology WILEY

PRIMARY RESEARCH ARTICLE

Retrospective analysis of wood anatomical traits and tree-ring isotopes suggests site-specific mechanisms triggering *Araucaria araucana* drought-induced dieback

Paulina F. Puchi[1] | J. Julio Camarero[2] | Giovanna Battipaglia[3] | Marco Carrer[1,4]

[1]Dipartimento Territorio e Sistemi Agro-Forestali (TESAF), Universitá degli Studi di Padova, Legnaro, PD, Italy

[2]Instituto Pirenaico de Ecología (IPE-CSIC), Zaragoza, Spain

[3]Department of Environmental, Biological and Pharmaceutical Sciences and Technologies, University of Campania 'L. Vanvitelli', Caserta, Italy

[4]Institute of Atmospheric Sciences and Climate, ISAC-CNR, Bologna, Italy

Correspondence
J. Julio Camarero, Instituto Pirenaico de Ecología (IPE-CSIC), 50080 Zaragoza, Spain.
Email: jjcamarero@ipe.csic.es

Funding information
Rufford Foundation, Grant/Award Number: Small Grant N°23677-1

Abstract

In 2010–2018, Northern Patagonia featured the longest severe drought of the last millennium. This extreme dry spell triggered widespread growth decline and forest dieback. Nonetheless, the roles played by the two major mechanisms driving dieback, hydraulic failure and carbon starvation, are still not clear and understudied in this seasonally dry region. Here, for the 1800–2017 period, we apply a retrospective analysis of radial growth, wood anatomical traits (lumen area, cell-wall thickness) and $\delta^{13}C$ and $\delta^{18}O$ stable isotopes to assess dieback causes of the iconic conifer *Araucaria araucana*. We selected three stands where declining (defoliated) and nondeclining (not defoliated) trees coexisted along a precipitation gradient from the warm-dry Coastal Range to the cool-wet Andes. At all sites declining trees showed lower radial growth and lower theoretical hydraulic conductivity, suggesting a long-lasting process of hydraulic deterioration in their water transport system compared to nondeclining, coexisting trees. Wood anatomical traits evidenced that this divergence between declining and nondeclining trees started at least seven decades before canopy dieback. In the drier stands, declining trees showed higher water-use efficiency (WUE) throughout the whole period, which we attributed to early stomatal closure, suggesting a greater carbon starvation risk consistent with thinner cell walls. In the wettest stand, we found the opposite pattern. Here, a reduction in WUE coupled with thicker cell walls suggested increased carbon assimilation rates and exposure to drought-induced hydraulic failure. The $\delta^{18}O$ values indicated different strategies of gas exchange between sites, which are likely a consequence of microsite conditions and water sources. Multiproxy, retrospective quantifications of xylem anatomical traits and tree-ring isotopes provide a robust tool to identify and forecast, which stands or trees will show dieback or, on the contrary, which will likely withstand and be more resilient to future hotter droughts.

KEYWORDS
Argentina, cell-wall thickness, Chile, climate change, drought, growth decline, hydraulic conductivity, lumen area, tree mortality, water-use efficiency

1 | INTRODUCTION

Hotter droughts, that is, droughts accompanied by warmer temperatures, in combination with altered disturbance regimes, have caused forest dieback, and increased tree mortality rates, modifying the structure and distribution of forests worldwide (Allen et al., 2010, 2015; Anderegg et al., 2013; McDowell et al., 2020). In addition, climatic models have predicted the frequency, intensity, and duration of such hotter droughts will increase in the next decades, and such events will be more severe in areas subjected to seasonal drought (Jia et al., 2019; Trenberth et al., 2014).

Hotter drought has negative impacts on physiological processes in forest ecosystems, constraining growth and promoting transpiration, inducing hydraulic failure via xylem embolism, and limiting the carbon sink capacity via stomatal closure (Bréda et al., 2006). Trees could become prone to growth decline, crown dieback, and death from two nonexclusive physiological mechanisms: hydraulic failure or carbon starvation (Adams et al., 2017; Hammond et al., 2019; McDowell et al., 2008). To better understand the long-term changes in growth and vigor and to improve our predictive capacity of dieback and tree death in response to hotter droughts in the future, it is crucial to identify which are the physiological mechanisms that allow trees to withstand and cope with severe water shortage (Brodribb et al., 2020; McDowell et al., 2020). The drought-induced cascading changes in tree function (e.g., loss in hydraulic conductivity, impaired carbon uptake) leading to dieback and tree mortality can be reconstructed by analyzing long-term changes in tree radial growth (Cailleret et al., 2016, 2019), wood-anatomical traits (e.g., conduits dimension) (Pellizzari et al., 2016), and intrinsic water-use efficiency (WUE_i), (Colangelo et al., 2017). These are some of the proxies of tree functioning, which may allow reconstructing and inferring the relative roles played by the two proposed mechanisms leading to dieback.

In the case of wood anatomy, traits such as lumen area (LA) (a proxy of theoretical hydraulic conductivity; Cuny et al., 2015) and cell-wall thickness (CWT) (a proxy for xylem carbon use; Castagneri et al., 2017, 2018) allow quantifying the long-term tree response to drought stress (Fonti et al., 2010). The evaluation of WUE_i, that is, the cost of fixing carbon in terms of water loss (Ehleringer et al., 1993), may be achieved by measuring carbon isotope discrimination in wood or cellulose ($\delta^{13}C$), which provides information about the ratio of net photosynthetic CO_2 assimilation rate (A) to stomatal conductance rate (g_s), which depends of temperature and vapor pressure deficit among other factors (Farquhar et al., 1982). Furthermore, the contribution of g_s in driving variation of WUEi is inferred by assessing the variation of $\delta^{18}O$ in tree rings, which depends on leaf transpiration and the evaporative enrichment of oxygen isotope ratios (Saurer et al., 2004; Scheidegger et al., 2000; Seibt et al., 2008). The combination of this dual-isotope approach has been adopted to better understand water and carbon limitations in drought-induce dieback studies (Cherubini et al., 2021; Colangelo et al., 2017; Petrucco et al., 2017; Timofeeva et al., 2017).

Hence, a multiproxy study of tree-ring width (TRW), wood anatomy, and WUE_i can provide new insights to disentangle the physiological mechanisms under drought conditions and to reconstruct long-term water-use strategies in trees (Gessler et al., 2018; Hentschel et al., 2014). Nonetheless, until now, this multifaceted approach has been hardly applied, and a clear and univocal interpretation of drought-induced dieback in many tree species is still lacking. For instance, some authors have observed in declining trees the reduction of LA, and this has been linked to reduced hydraulic conductivity (Liang et al., 2013; Pellizzari et al., 2016). Others have found the opposite, interpreting that fast-growing trees, producing wider lumens in stressful conditions, were more prone to xylem embolism and declined (Petrucco et al., 2017; Voltas et al., 2013). Related to tree growth, Cailleret et al. (2019) compared radial growth trends and rates in coexisting surviving and dead trees, and they observed in gymnosperms a drastic reduction of radial growth 20 years before mortality; however, other studies found the opposite, that is, declining trees were fairly fast-growing before the drought started (Hentschel et al., 2014; Voltas et al., 2013). Finally, recent studies have shown an increase of WUE_i in declining trees (Timofeeva et al., 2017). However, until now, there is no consensus about the mechanisms triggering changes in growth, vigor and causing dieback and mortality (Brodribb et al., 2020; Gessler et al., 2018; Trugman et al., 2021). It is, therefore, possible that the relative importance of mechanisms leading to dieback is reliant on site-specific conditions, which requires studying sites subjected to contrasting climatic conditions.

In South America, several temperate tree species showed abrupt growth reductions and mortality events in response to 20th-century warming and drying trends across Patagonia (Cailleret et al., 2016; Villalba et al., 2012). Several studies carried out in Argentina and Chile have shown die-off phenomena affecting *Nothofagus* species and some conifers such as *Austrocedrus chilensis* (Amoroso et al., 2012; Miranda et al., 2020; Serrano-León & Christie, 2020; Suarez et al., 2004). Here, we argue how a multiproxy approach, combining analysis of wood anatomical traits and stable isotopes in tree-rings, can be leveraged for a comprehensive interpretation of the physiological mechanisms involved in forest dieback. This is the first study to investigate, in the iconic and threatened conifer species *Araucaria araucana* (Molina) K. Koch, the causes of drought-induced dieback by retrospectively analyzing an assemblage of wood traits, that is, long-time series of tree growth, wood-anatomical traits, and tree-ring stables isotopes in coexisting nondeclining and declining trees, and along a precipitation gradient in Northern Patagonia. In the last decades, this region experienced very dry conditions in 1998, linked to La Niña event (Muñoz et al., 2016), and the longest drought (2010–2018) of the last millennium (Garreaud et al., 2019). These and previous dry spells impacted Northern Patagonia forests in several ways by increasing canopy dieback incidence, tree mortality rates and enhancing wildfire occurrence (Kitzberger et al., 2001; Villalba & Veblen, 1998). Here, we hypothesize that declining and dying trees, showing higher percentage of crown defoliation, could be characterized by reduced tree-ring growth and lower hydraulic conductivity than coexisting nondeclining trees. Specifically, we expect that declining trees will produce smaller LA (mirroring water shortage during tracheid enlargement) and thinner CWT (reflecting depletion

of carbon reserves due to reduced photosynthetic and cell-wall lignification rates) than nondeclining trees. We also expect that declining trees will present a higher WUE_i, due to reduced water loss per unit carbon gain, compared to nondeclining trees. Investigating how trees respond to long-term warming conditions and drought will help us to disentangle the physiological mechanisms and WUE_i strategies to infer causal links between drought, dieback, and tree death. This knowledge has the potential to predict which tree populations will significantly decline or, on the contrary, which stands will be able to withstand and be more resilient to future climate warming (Pellizzari et al., 2016). Such tools are urgently needed for threatened species such as *A. araucana*, with highly endangered provenances inhabiting the driest sites of its distribution area (Premoli et al., 2013).

2 | MATERIALS AND METHODS

2.1 | Tree species and geographical distribution

Araucaria araucana (Molina) K. Koch is an endemic evergreen conifer of the temperate forests of South America. This tree is the second long-lived species of South America and can reach ages of 1000 years (Aguilera-Betti et al., 2017). The distribution area of *A. araucana* (37°20′–40°20′S; Figure 1) includes the Andes range (between 900 and 1700 m a.s.l.) and the Chilean Coastal range (between 850 and 1400 m a.s.l.) (Veblen et al., 1995).

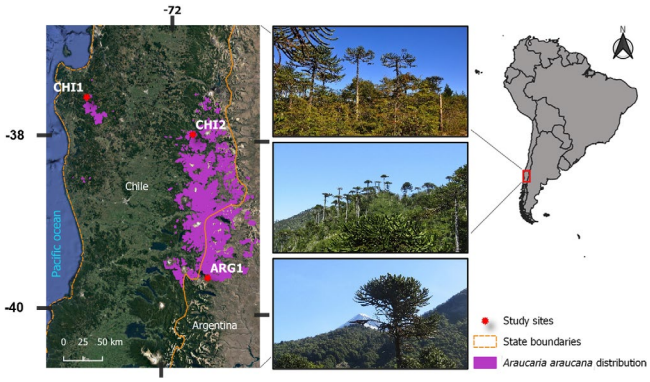

FIGURE 1 *Araucaria araucana* natural distribution (purple areas). Location of the three study sites in temperate rainforest in northern Patagonia, including southern Chile and south-western Argentina (red stars). Images show sampled sites

Araucaria araucana is a dioecious conifer, which can reach up to 40 m in height, forming a thick and straight cylindrical trunk up to 2 m in diameter. Nowadays, the species is classified as endangered, due to extensive logging and human-induced fires (Premoli et al., 2013).

2.2 | Study sites and climate

In January 2019 (austral summer), we selected three sites dominated by *A. araucana* affected by the 2010–2018 drought (Garreaud et al., 2019) with a high percentage of canopy defoliation, leaves discoloration and branch dieback and abundant dying trees.

Sites were selected across the natural distribution of *A. araucana* in the Chilean Coastal range and the Andes range in the border between Chile and Argentina (Figure 1; Table 1). The sites were Trongol Alto (hereafter abbreviated as CHI1), Altos de Pemehue National Reserve (hereafter abbreviated as CHI2), both located in Chile, and Tromen Lake situated in Argentina (hereafter abbreviated as ARG1). All sites were located within conservation areas. Sites selection allowed the comparison along a marked precipitation gradient since rainfall increases eastwards and upwards. Moving from north to south, the average annual temperature is 13.0° to 11.7°C and the mean yearly precipitation ranges from 1091 to 3002 mm (Figure S1). All locations show the typical temperate rainforest climate characterized by wet winters and hot summers with a more marked summer drought at CHI1. In the Andes CHI2 and ARG1 sites, the soil is shallow, composed by volcanic ash and scoria characterized by low water holding capacity and deficient nutritional levels. On the other hand, in the coastal range site (CHI1), soils are usually shallow but poor-drained and develop on granitic and metamorphic bedrocks (CIREN, 2010). All sites present signs of not recent (more than 50–100 years) natural or anthropogenic disturbances mostly in terms of fires and logging.

2.3 | Field sampling

The three sites were dominated by *A. araucana* old-growth forests with abundant mature trees and heterogeneous vertical and horizontal structures. We randomly selected trees firstly defining their health status according to crown condition by estimating the percentage of crown defoliation of each tree using binoculars. Trees presenting crown defoliation <50% were categorized as nondeclining individuals, while trees with crown defoliation ≥50% were

TABLE 1 Geographical and mean annual climate characteristics for the three sites

Site	Country	Latitude (S)	Longitude (W)	Altitude (m a.s.l.)	Mean minimum annual temperature (°C)	Mean annual temperature (°C)	Mean maximum annual temperature (°C)	Annual precipitation (mm)
CHI1	Chile	37°33′	73°13′	980	7.9	13.0	18.0	1091
CHI2	Chile	37°57′	71°39′	1370	3.8	12.2	17.2	2069
ARG1	Argentina	39°36′	71°21′	1020	3.5	11.7	15.9	3002

TABLE 2 Mean biometric parameters of the *Araucaria araucana* nondeclining and declining trees analyzed per site. Data are means ± SE

	Nondeclining trees			Declining trees		
Variable	**CHI1**	**CHI2**	**ARG1**	**CHI1**	**CHI2**	**ARG1**
No. of trees	9	9	12	7	6	11
Height (m)	12.0 ± 1.2	18.3 ± 1.8	14.6 ± 1.9	10.7 ± 1.4 b	15.7 ± 3.0	12.7 ± 1.1
DBH (cm)	45.6 ± 3.9	62.8 ± 6	73.9 ± 10.3	36.4 ± 3.1	51.1 ± 9.4	53.6 ± 6.7
Tree-ring width (mm)	0.54 ± 0.14 a	0.55 ± 0.16 a	0.90 ± 0.17 a	0.47 ± 0.16 b	0.35 ± 0.08 b	0.79 ± 0.17 b
Age at 1.3 m (years)	198 ± 29	335 ± 34.7	226 ± 39.3	163 ± 19.7	332 ± 40	249 ± 31.7
Defoliation (%)	28.3 ± 3.5 a	9.4 ± 5.1 a	27.9 ± 3.7 a	67.9 ± 4.6 b	79.2 ± 7.3 b	73.2 ± 4.3 b

Different letters indicate significant differences ($p < .05$) between nondeclining and declining trees of the same site based on Mann-Whitney test.

considered declining (Camarero et al., 2015). Then, after having identified a declining individual, we selected a healthy one with similar dimensions as close as possible to the first one. We finally selected 54 trees (27 couples) and for each tree, after defining the defoliation status, we measured diameter at breast height (measured at 1.3 m) and height (using a laser rangefinder), and collected two 10-mm cores per tree with an increment borer (Table 2).

2.4 | Climate data

Daily climate records of rainfall, minimum, mean, and maximum temperature, for each site were obtained from the Chilean Directorate of water resources (DGA), and National Weather Service (DMC; Table S1 and Figure S1). All the station data are available from the Research Center for Climate Science and Resilience (http://explorador.cr2.cl).

In addition, to quantify drought severity, we calculated the Standardized Precipitation-Evapotranspiration Index (SPEI), which provides climate water balance (precipitation—potential evapotranspiration) (Vicente-Serrano et al., 2010). The drought severity index was computed at different time scales (from 1 to 20 months) for the 1950–2017 period in R using the package SPEI (Beguería et al., 2014).

2.5 | Processing of wood samples

Once back in the laboratory, cores were air dried, polished with successive grains to make the ring boundaries visible at best, and then ring widths were measured to a precision of 0.01 mm using the TSAP measuring device (Rinntech). Then the tree-ring series were visually cross-dated using standard dendrochronological methods (Stokes & Smiley, 1968), and checked for dating accuracy and measurement errors with the COFECHA program (Holmes, 1983). For dating purposes, we followed the convention for the Southern Hemisphere, which assigns to each ring the date of the year in which growth started (Schulman, 1956). Finally, we defined the age of each tree as the sum of the number of years from the cross-dated cores plus the number of rings estimated with pith-offset (the difference in years between the innermost dated ring in a core and the pith at sampling level) (Norton et al., 1987).

For cell anatomical analysis, we selected 10 cores per site, five from nondeclining trees and five from declining trees, avoiding cores with scars, rotten wood, or missing parts. The selected trees were those showing the highest correlation with the mean series of nondeclining and declining trees in each site. For anatomical measurements we followed the standard protocol proposed by von Arx et al. (2016), which involves (i) splitting each core in 3–4-cm-long pieces, (ii) cutting 12-μm thick cross-sections with a rotary microtome (Leica), (iii) staining them with a solution with safranin (1%) and Astra blue (0.5%), (iv) permanently fixing the slices on microscopic glass slides using Eukitt (Bio Optica), and (v) scanning each slide at 100× magnification using a digital automated microscope (D-sight; Menarini Diagnostic). Cell anatomical traits were measured and processed with ROXAS, an image analysis software that uses the commercial software Image-Pro Plus v.6.1 to process images (Media Cybernetics). This software provides detailed measurements of many traits: TRW, number of cells (CN) per ring, transversal LA, lumen diameter (LD), theoretical hydraulic conductivity (K_h), hydraulic diameter (D_h), cell diameter (CD), CWT (measured along the radial—CWT_{RAD}—and tangential—CWT_{TAN}—directions, and considering their mean value CWT_{ALL}), cell total area (CTA), and the relative position of each element within the annual ring, among others (von Arx & Carrer, 2014; Prendin et al., 2017). These variables were measured along 10-mm tangential windows encompassing the whole ring. In total, 7800 rings (CHI1: 2208; CHI2: 3312; ARG1: 2280) and more than 15,000,000 tracheids were analyzed from the period 1449 to 2017 (Table 2).

2.6 | Wood anatomy data

Both TRW and anatomical trait series were standardized by removing the size/age trends using a 32-year cubic smoothing spline, to stabilize the variance and preserve high to decadal frequency variability potentially related to climate (Carrer et al., 2015; Cook & Kairiukstis, 1990). To accomplish this step, individual series were detrended fitting the spline curve to measured data series and then

dividing observed by expected values. The resulting dimensionless indexes were then averaged at site level for each vigor class using a biweight robust mean (Cook & Kairiukstis, 1990). Then, raw and standardized chronologies for anatomical traits of CN, LA, LD, K_h, D_h, CD, CWT, CWA, and CTA were computed with dplR package in R (Bunn, 2008; Bunn et al., 2021; R Core Team, 2021). We assessed the common variability between trees by calculating, for the time series of the selected variables (TRW, LA, K_h, and CWT), the mean correlation (rbar) values and the common variance considering the common period 1900–2017 (Table S2).

Later, for the selection of the most representative xylem traits that can be highly correlated among them, we performed at site level a principal component analysis (PCA) (Jolliffe, 2002) based on a correlation matrix of growth and anatomical variables (TRW, CN, LA, LD, D_h, K_h, CWT_{RAD}, CWT_{TAN}, CWA) and considering the 1950–2017 period, which is the same time interval adopted to assess the climate-growth associations. The significance of the principal components was verified with a randomization test and applying the lambda stopping rule (Peres-Neto et al., 2005). Scatter plots of the weighting coefficients for the first two principal components (PC1 and PC2) were used to display the similarities among variables.

2.7 | Stable isotope analyses

The carbon and oxygen isotope analyses were performed on the same trees used for wood-anatomical analyses. We used rings spanning the period 1800–2017 and split the cores with a scalpel under a binocular in decadal wood segments (e.g., 1800–1809, 1810–1819, …, excepting 2010–2017). In total, we obtained 22 samples per tree. The same chronological decadal segments were pooled together at site level, milled to a fine powder with a ball mill (ZM 1000; Retsch) and weighed 0.05–0.06 mg and 0.08–0.09 mg of wood for carbon and oxygen isotope analyses, and, finally, encapsulated in tin and silver capsules, respectively.

The isotope composition was measured at the IRMS laboratory of the University of Campania "Luigi Vanvitelli" by using mass spectrometry with continuous flow isotope ratio (Delta V plus Thermo electron Corporation). Standard deviation for repeated analysis of an internal standard (commercial cellulose) was better than 0.1‰ for carbon and better than 0.3‰ for oxygen. The $\delta^{13}C$ series were corrected for the fossil fuel combustion effect (Francey et al., 1999).

2.8 | WUE_i inferred from carbon isotope discrimination

Measurements of $\delta^{13}C$ were used to calculate intrinsic WUE_i for nondeclining and declining trees. WUE_i is defined as the ratio between the net photosynthesis rate (A) and the stomatal conductance to water vapor (g_s) rate (Ehleringer et al., 1993) and computed as:

$$WUE_i = A/g_s = (c_a - c_i)/1.6, \quad (1)$$

where c_a is the concentration of CO_2 in the atmosphere; c_i is the concentration of CO_2 in the intercellular spaces; and 1.6 is the ratio of water and CO_2 diffusivity in the atmosphere.

For *A. araucana*, WUE_i can be calculated starting from the $\delta^{13}C$ of the plant material ($\delta^{13}C_{tree}$), which is related to atmospheric $\delta^{13}C$ ($\delta^{13}C_{atm}$) and to the ratio c_i/c_a, according to Farquhar and Richards (1984) and Farquhar et al. (1982):

$$\delta^{13}C_{tree} = \delta^{13}C_{atm} - a - \left[(b-a)\,c_i\right]/c_a, \quad (2)$$

where a is the fractionation factor due to $^{13}CO_2$ diffusion through stomata (4.4‰), and b is the fractionation factor due to Rubisco enzyme during the process of carboxylation (27‰). Therefore, we can calculate c_i by using the formula:

$$c_i = c_a(\delta^{13}C_{atm} - \delta^{13}C_{tree} - a)/(b-a). \quad (3)$$

Finally, the WUE_i can be calculated as follows:

$$WUE_i = (c_a b - \delta^{13}C_{atm} + \delta^{13}C_{tree})/1.6\,(b-a). \quad (4)$$

However, the WUE_i should not be considered as equivalent to instantaneous WUE, which is the ratio of assimilation (carbon gained) to transpiration (water lost) and takes into account the atmospheric water demand (Pacheco et al., 2020; Seibt et al., 2008). Thus, the equation used is the "simple" form of isotopic discrimination that does not include effects due to mesophyll conductance and photorespiration, which were not available for the study species.

We used $\delta^{13}C_{atm}$ values for the period 1850–2017 from Belmecheri and Lavergne (2020). We obtained the atmospheric concentration of CO_2 from the Mauna Loa station data (available at http://www.esrl.noaa.gov/) and for the period before 1850 from the ice cores obtained at Law Dome, East Antarctica (http://cdiac.ornl.gov/trends/co2/lawdome.html).

2.9 | Statistical analyses

To compare mean values of the analyzed variables (TRW, wood anatomy traits, WUE_i, and $\delta^{18}O$) between the two vigor classes at each site we used the Mann-Whitney U tests and the paired-sample t test. The statistical significance between tree growth, wood-anatomical traits and isotopes data were tested using Pearson correlations. We used the Wilcoxon rank-sum test to check if the changes through time of growth (TRW) and wood anatomical variables or isotope ratios differed between nondeclining and declining trees (Hentschel et al., 2014).

Associations between climate variables and standardized series of growth indices and wood anatomical traits were assessed by calculating Pearson correlations from prior September to current April (growing season in the Southern Hemisphere) and considering the period 1950–2017.

3 | RESULTS

3.1 | Traits selection

PCA was performed with the chronologies of growth, and xylem anatomical traits were resulted for all the sites in two significant principal components (PC1 and PC2): together they explained 80.2%, 82.4%, and 83.1% of the variance for CHI1, CHI2, and ARG1 sites, respectively (Figure 2). The ordination along the two axis revealed recurrent patterns with three groups corresponding to (i) hydraulic traits (LA, LD, K_h, D_h, and CTA) showing high PC1 scores, (ii) growth traits (TRW and CN) showing high PC2 scores, and (iii) traits related to carbon use (CWT_{RAD}, CWT_{TAN}, CWT_{ALL} and CWA) with low PC1 scores. According to these outcomes, we selected TRW, LA and K_h, and CWT_{ALL} as representative traits for each of these groups.

3.2 | Climate trends and drought variability

Annual precipitation showed a significant reduction (Figure S2) at sites CHI1 and CHI2 from 1950 to 2017. At the same time, mean temperature showed a significant increase in the CHI2 and ARG1 sites located at the Andes range.

Drought severity significantly intensified in all sites (Figure 3). The SPEI drought index showed that the driest coastal range site CHI1 was severely impacted by the 2010–2018 drought (Figure 3), whereas the wettest site ARG1, was mostly affected by the severe 1998 drought (Figure 3).

3.3 | Biometric parameters, growth, and wood anatomical traits

Declining trees presented significantly narrower rings than nondeclining trees (Table 2). Growth rate (TRW) usually showed higher mean intertree correlation (rbar) and common variance than woodanatomical variables such as LA, K_h, and CWT (Table S2). We found a drastic growth reduction starting more than 120, 50, and 80 years ago in declining trees from CHI1, CHI2, and ARG1 sites, respectively (Figure 4a). The TRW and its cell number were positively related. Nonetheless, in all sites, trees of the two vigor classes were similar in terms of diameter, height, and age (Table 3) and also showed similar year-to-year variability in the TRW chronologies (Figure S3).

During the 1800–2017 period, as for TRW, CN is significantly lower for declining trees in all sites (Table 3; Figure 4b), whereas tracheids in declining trees presented a clear smaller LA than nondeclining trees in CHI1 and ARG1 sites. This pattern was more evident at the driest site CHI1. In CHI2 site, LAs were rather similar.

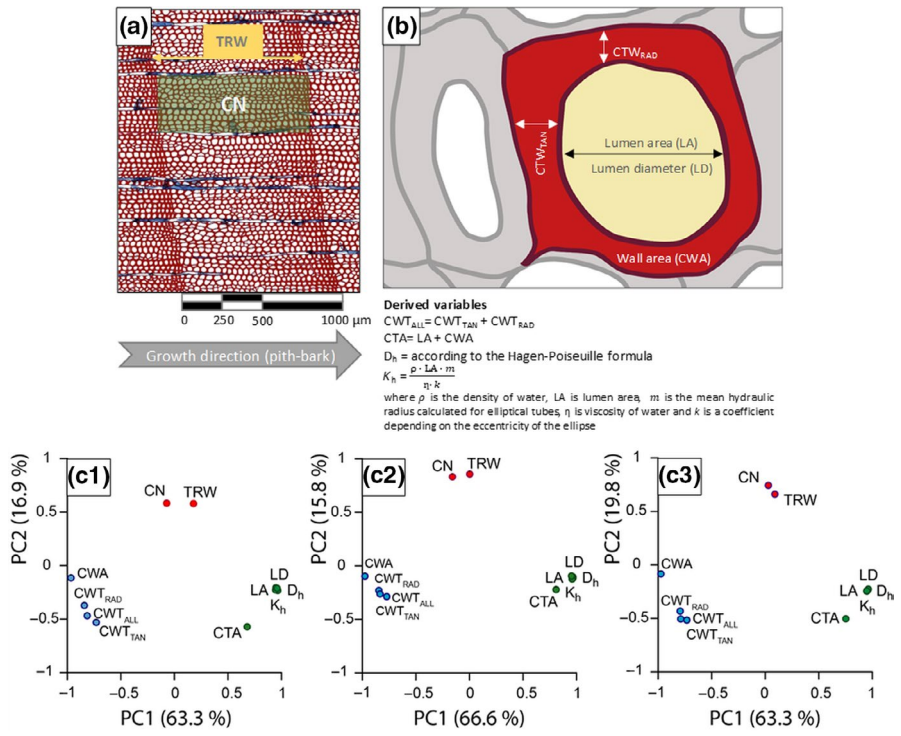

FIGURE 2 View of *Araucaria araucana* tree ring and illustration of the growth (a, TRW, tree ring width; CN, cell number along the radial direction) and anatomical traits (b, LA, lumen area; LD, lumen diameter, Dh, hydraulic diameter; Kh, theoretical hydraulic conductivity; CWTRAD, radial cell wall thickness; CWTTAN, tangential cell wall thickness, CWTALL, total cell wall thickness; CWA, cell wall area; and CTA, cell total area) considered. Scatter plots of the scores for the first (PC1) and second (PC2) principal components calculated on growth and anatomical traits chronologies for the CHI1, CHI2 and ARG1 sites (c1–c3)

Consequently, the theoretical hydraulic conductivity (K_h) was also lower in declining trees, indicating a theoretically lower water transport capacity than nondeclining trees (Table 3; Figure 4c). LA in the CHI2 site presented lower mean values compared with CHI1 and ARG1 sites (Table 3; Figure 4b,c).

Finally, CWT was thinner in declining trees at the CHI1 and CHI2 sites throughout the whole period, indicating a potential limitation in their carbon use to build cell walls. On the contrary, in the ARG1 site, we observed an increase in CWT starting in the 20th century (Figure 4d).

Considering all growth and anatomical traits, Pearson correlations were positive among traits related to LA (LD, LA, D_h, CTA, K_h), but they were negatively related to cell-wall traits (CWT, CTA) (Figure S4). These results were in agreement with the PCA (Figure 2).

3.4 | Growth and wood anatomical traits associations with climate variables

Growth and wood anatomical traits of the two vigor classes showed significant correlations with climate variables and SPEI in all study sites (Figure S5). In general, TRW, LA, and K_h were negatively correlated with growing season temperature (September–April), and positively related with summer precipitation and SPEI (December–February, Figure S5). At CHI1, growth (TRW) of declining trees was negatively correlated with maximum temperature from November to February and positively correlated with February precipitation in both tree groups. Similarly, December precipitation was positively related to LA and K_h in declining trees, and this relationship was stronger in nondeclining than in declining trees. The same pattern was observed with SPEI during summer (Figure S5).

At CHI2, TRW of nondeclining and declining trees was negatively associated with minimum and maximum temperatures during the growing season (Figure S5). In this site, TRW, LA, and K_h showed the weakest correlations with precipitation and SPEI (Figure S5).

At ARG1, TRW showed a positive association with precipitation (December and March) and growing-season SPEI. LA and K_h of nondeclining trees were negatively related to the minimum temperature of February but positively related to precipitation of October, November, and February. LA and K_h were correlated with growing season SPEI (Figure S5).

Overall, CWT in nondeclining trees showed positive correlations with growing season maximum temperature, whereas in declining trees there were positive correlations with maximum temperature at the beginning of the growing season (October) in CHI1 and ARG1 sites. On the contrary, CWT showed a negative correlation with spring precipitation and summer SPEI, which was particularly strong in the ARG1 site (Figure S5).

In CHI1 and ARG1 sites, the highest correlations between tree-ring and anatomical variables and climate were found for SPEI (Figure S5). Overall, LA and K_h, showed a greater positive influence of growing season precipitation and SPEI at CHI1 and ARG1 sites, suggesting a higher sensitivity to soil moisture conditions. On the other hand, growing season temperature was positively related to TRW at the CHI2 site, suggesting a moderate water shortage constraining growth at this site.

3.5 | Patterns of WUE_i and $\delta^{18}O$

In all sites, the increasing trend in WUE_i for both tree vigor classes started in 1850 (Figure 5). The increase of WUE_i in the period was linearly associated with the increase in atmospheric CO_2 concentrations

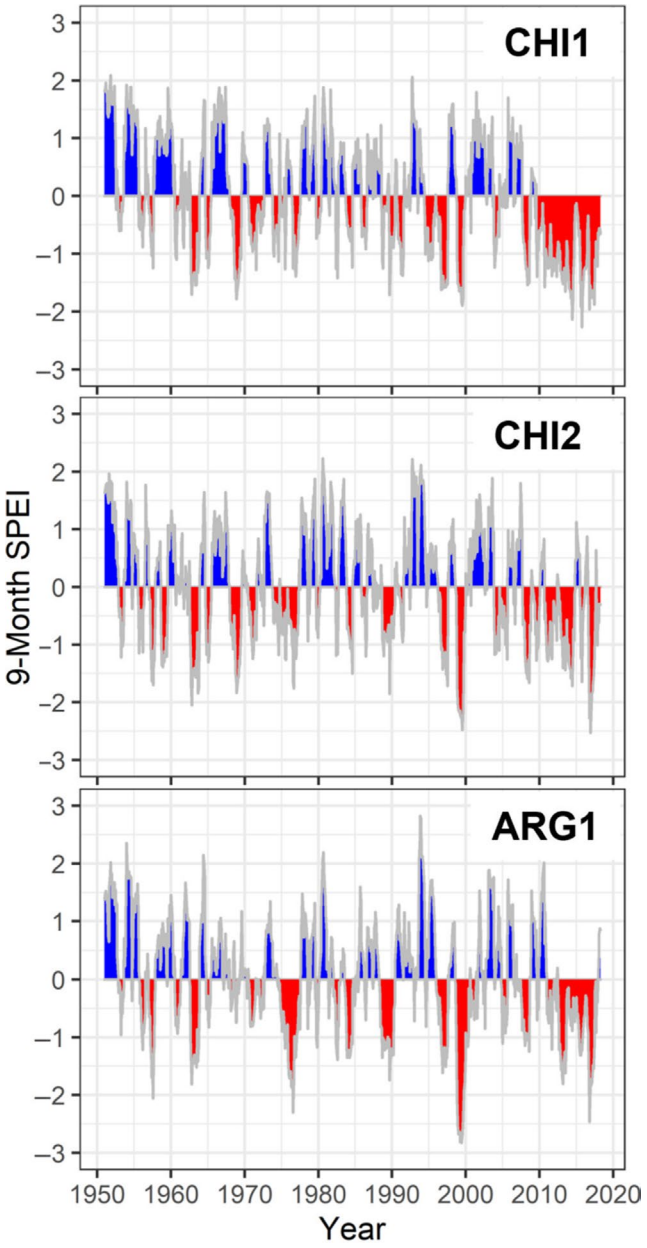

FIGURE 3 Standardized 9-month SPEI at the three study sites (CHI1, CHI2 and ARG1) for the 1950–2017 period. Negative (red) and positive (blue) values indicate drier and wetter conditions, respectively

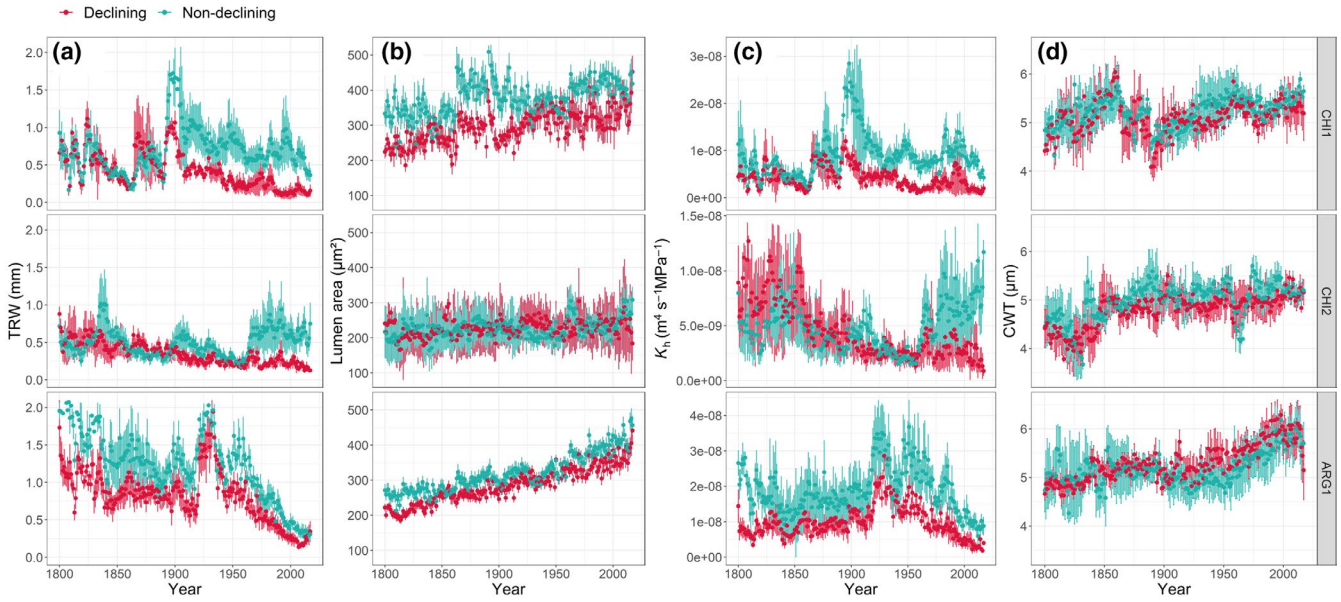

FIGURE 4 (a) Tree-ring width (TRW), (b) tracheid lumen area (LA), (c) theoretical hydraulic conductivity (Kh) and (d) cell-wall thickness (CWT), for non-declining (green line) and declining (red line) *Araucaria araucana* trees in the three study sites (CHI1, CHI2 and ARG1), during the period 1800–2017 (note the different site-related scale for Kh). Values are means ± SE

TABLE 3 Statistics of wood-anatomical variables in the *Araucaria araucana* nondeclining and declining trees. Data are means ± SE and correspond to the 1800–2017 period

	Nondeclining trees			Declining trees		
Variable	**CHI1**	**CHI2**	**ARG1**	**CHI1**	**CHI2**	**ARG1**
Lumen area (μm^2)	317.3 ± 5.4 a	227.3 ± 5.4	298.1 ± 6.6	249.3 ± 4.22 b	226.8 ± 7.0	288.3 ± 5.23
Cell-wall thickness (µm)	5.3 ± 0.03 a	5.2 ± 0.04 a	5.3 ± 0.03 a	4.9 ± 0.03 b	4.8 ± 0.04 b	5.4 ± 0.03 b
K_h ($m^4\ s^{-1}\ MPa^{-1}$)	$8.1e^{-9} \pm 2.9e^{-10}$ a	$1.9e^{-8} \pm 1.3\ e^{-10}$ a	$1.9\ e^{-8} \pm 4.5\ e^{-10}$ a	$3.8\ e^{-9} \pm 1.5e^{-10}$ b	$4.5\ e^{-9} \pm 1.7e^{-10}$ b	$1.0\ e^{-8} \pm 3.1\ e^{-10}$ b
Cell number per ring (*n*)	1538 ± 49 a	1756 ± 44 a	3710 ± 130 a	1324 ± 54 b	1490 ± 61 b	2586 ± 94 b

Abbreviation: K_h, theoretical hydraulic conductivity.

Different letters indicate significantly different values ($p < .05$) between nondeclining and declining trees of the same site based on Mann-Whitney tests.

($p < .05$). The mean WUE_i derived in declining trees presented significant higher values than nondeclining trees in the drier CHI1 and CHI2 sites (Table 4). In the more humid ARG1 site, declining trees showed higher WUE_i only at the beginning of the 19th century, but this pattern reversed after the 1980s, although the mean WUE_i values in both vigor classes did not present significant differences (Table 4). Declining trees in all the sites and for the whole 1800–2017 period featured significant higher $\delta^{18}O$ values than nondeclining trees. This pattern was more evident in the CHI1 and CHI2 sites (Figure 5).

The relationship between $\delta^{13}C$ and $\delta^{18}O$ was always positive for both vigor classes; however, the linear trend was not significant for both groups in the ARG1 site and just for the nondeclining trees in the CHI2 site. In the CHI1 site we found the strongest $\delta^{13}C$–$\delta^{18}O$ association (Figure 6).

The precipitation of February was positively correlated with $\delta^{13}C$ in declining trees in all sites (Figure S6). The $\delta^{13}C$ and $\delta^{18}O$ series of two vigor classes were negatively correlated with temperature in CHI2 and ARG1 sites during the growing season. Instead, in the CHI1 site nondeclining trees presented a negative correlation with $\delta^{13}C$ during summer and a positive correlation with $\delta^{18}O$ (Figure S6).

4 | DISCUSSION

The recent 2010–2018 drought that affected Chile in the early 21st century suggested Northern Patagonia may become a climate change hotspot (Garreaud et al., 2019). With this study, our goal was to elucidate the causes of *A. araucana* dieback as related to recent dry spells in the region. We applied a retrospective multiproxy approach analyzing several traits on three sites across a precipitation gradient and compared two groups of trees of different vigour but coexisting within the same stand and showing divergent responses

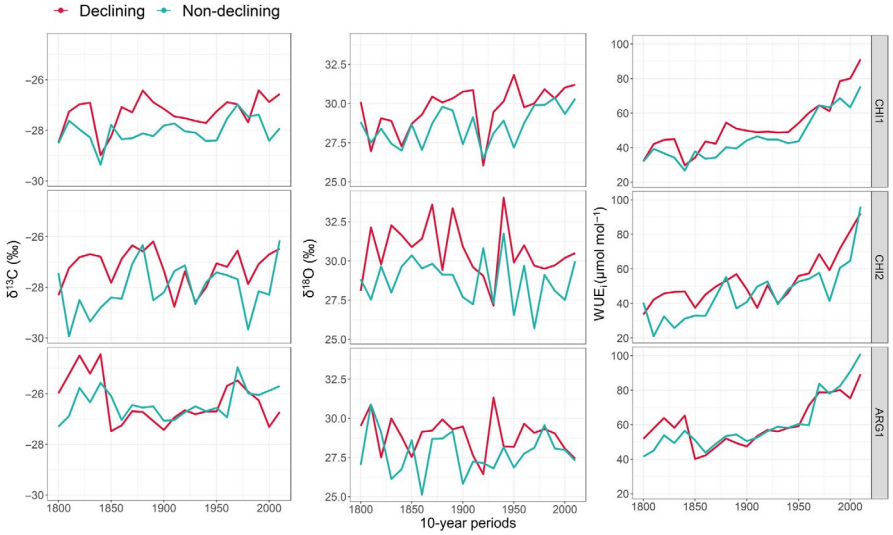

FIGURE 5 Patterns and trends in carbon (δ13C) and oxygen (δ18O) isotopes ratios of tree-ring and intrinsic water-use efficiency (WUEi) of non-declining (green lines) and declining (red lines) trees per site for the period 1800–2017. Values correspond to means for 10-year ring segments ($n = 22$)

TABLE 4 Statistics describing mean values of carbon ($\delta^{13}C$) and oxygen ($\delta^{18}O$) stable isotopes and intrinsic water-use efficiency (WUE_i) of nondeclining and declining trees per sites. Data are means ± SE and correspond to the mean for 10-year ring segments for the 1800–2017 period (n = 22 samples per site)

	$\delta^{13}C$ (‰)		$\delta^{18}O$ (‰)		WUE_i (µmol mol^{-1})	
Site	Nondeclining	Declining	Nondeclining	Declining	Nondeclining	Declining
CHI1	−28.03 ± 0.11a	−27.30 ± 0.14b	27.58 ± 0.25a	29.70 ± 0.31b	45.89 ± 2.8a	52.46 ± 3.3b
CHI2	−28.04 ± 0.21a	−27.21 ± 0.16b	28.77 ± 0.31a	30.63 ± 0.37b	45.96 ± 3.4a	53.06 ± 3.1b
ARG1	−26.39 ± 0.12	−26.33 ± 0.19	27.77 ± 0.28a	28.90 ± 0.25b	60.46 ± 3.4	60.56 ± 2.8

Different letters indicate significantly different values ($p < .05$) between nondeclining and declining trees of the same site based on paired-sample t tests.

to similar stressful climatic conditions. Our findings confirm that the drought-induced dieback can be the final step to the very long aftermath of the hydraulic deterioration and growth declining process.

4.1 | Growth and wood anatomical traits: early-warning signals of dieback

Through the retrospective examination of more than 200 years of growth and wood-anatomical traits, we showed that drought severity, expressed as SPEI, was the strongest climatic driver of tree growth, LA and K_h long-term variability both for nondeclining and declining trees. It is well known that during the growing season cell expansion highly depends on water availability and cell turgor, and therefore a drought period can strongly affect this crucial phase of cell development (Cuny et al., 2018). Warm spring–summer temperatures had a positive effect on CWT, as already observed in conifers (Björklund et al., 2021; Carrer et al., 2018). Hence, the increase of drought severity and intensity will have a first detrimental effect with the reduction of LA that will reduce hydraulic conductivity and constrain water transport capacity and growth (Pellizzari et al., 2016; Puchi et al., 2019), predisposing to dieback and mortality (McDowell et al., 2008).

Nonetheless, not all the trees within a stand responded in the same way, and, currently, declining trees resulted more sensitive to drought producing narrower tree rings and tracheids of smaller LA. The parallel drop of these two traits induced a dramatic reduction in the theoretical hydraulic conductivity (K_h). In addition, we demonstrated that the divergence in TRW and K_h between nondeclining and declining trees occurred in all sites many decades earlier than the recent 2010–2018 drought (Garreaud et al., 2019), and before any sign of decline such as leaf shedding or canopy dieback (Camarero et al., 2015; Pellizzari et al., 2016). Therefore, these two traits could be used as useful early-warning signals of tree death for this species. Such growth declines and the related loss in hydraulic conductivity anticipating a widespread forest dieback seems a recurring attribute at the driest distribution limits of many conifers sensitive to water shortage: a similar pattern was, for example, found in *Pinus sylvestris* and *Abies alba* in Spain (Pellizzari et al., 2016). In addition, previous studies in Patagonian temperate forests found a drastic reduction

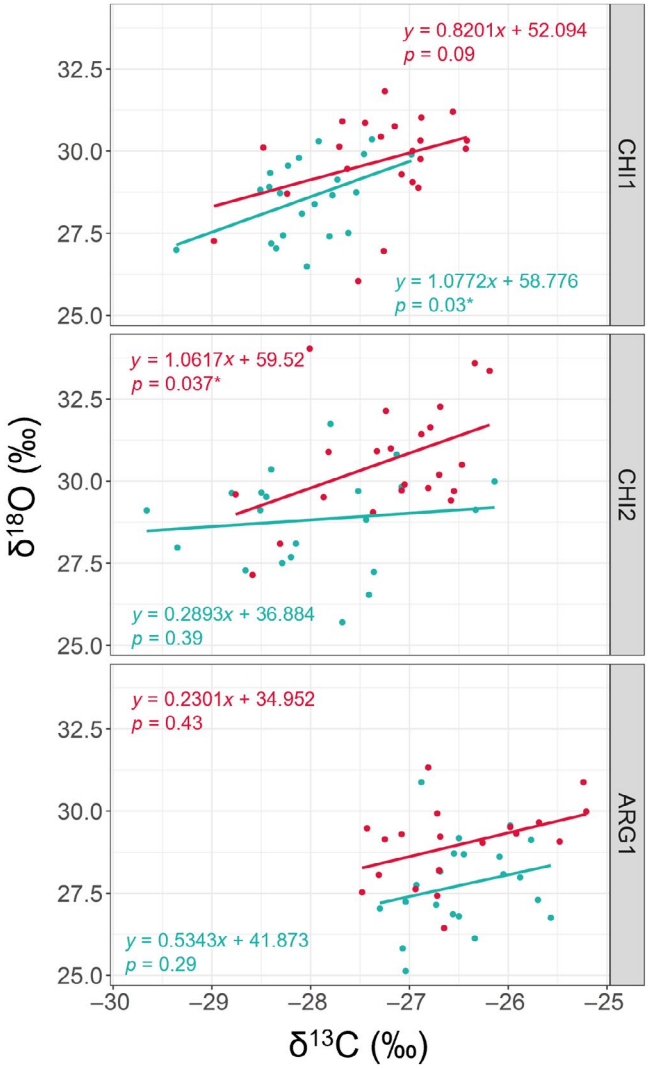

FIGURE 6 Relationships between carbon (δ13C) and oxygen (δ18O) isotopes ratios considering non-declining (red dots) and declining (green dots) *Araucaria araucana* trees in the three study sites. The lines show linear regressions and their corresponding equations are shown with the same colors

of growth in *A. araucana* and other species (*A. chilensis*, *Nothofagus betuloides*) since 1950, which was attributed to a positive increasing trend in the Southern Annular Mode leading to warmer and drier climate conditions (Villalba et al., 2012).

4.2 | Isotope signals for assessing forest dieback

Araucaria araucana is an extreme isohydric species (Zimmer et al., 2015), i.e. this species reduces stomatal conductance rates as soil water potential decreases and atmospheric conditions dry (Brodribb et al., 2004; McDowell et al., 2008). As we expected, declining trees presented higher WUE_i than nondeclining trees, but this was observed only at the driest Chilean sites. In Chile, declining trees had lower growth rates and K_h, together with higher WUE_i and $\delta^{18}O$. This indicates the closing of stomata to prevent water loss (Hentschel et al., 2014), but also incurs in an increased risk of carbon starvation (Gessler et al., 2018). The thinner cell walls of declining trees would agree with this interpretation indicating a lower carbon availability to build thicker walls. Indeed, although growth is not fully supplied by recent photosynthates, but also by carbon fixed in previous years (von Arx et al., 2017; Kagawa et al., 2006; Kuptz et al., 2011), several investigations confirmed that conifers rely much less and for less years on carbon reserves than broadleaves for xylem formation (Castagneri et al., 2018; Soudant et al., 2016; Zweifel et al., 2006).

Furthermore, the simultaneous analysis of tree-ring carbon and oxygen isotopes may help understanding the ecophysiological responses of trees in different sites, in particular to discriminate whether changes observed in WUE_i originated from a modification of *A* or g_s (Barbour, 2007; Dawson et al., 2002). Moreover, the positive correlation between WUE_i and $\delta^{18}O$ found in the Chilean sites suggests that declining trees experienced very tight stomatal control of leaf water loss during drought periods (Drake & Franks, 2003; Moreno-Gutiérrez et al., 2012; Petrucco et al., 2017). Therefore, the $\delta^{18}O$ increases in tandem with WUE_i, should confirm stomatal closure as the key driver of growth decline in the dry Chilean sites (Scheidegger et al., 2000). However, the different $\delta^{18}O$ values reported between declining and nondeclining trees could be linked to different water uptake ability, with declining trees being relatively better in exploiting the evaporative $\delta^{18}O$-enriched water from shallow soil layers (Battipaglia et al., 2010; Moreno-Gutiérrez et al., 2012). In contrast, nondeclining trees could uptake deeper water sources by forming deeper or more efficient root systems (Ripullone et al., 2020).

On the other hand, the WUE_i trends of declining and nondeclining trees were similar in the ARG1 site, suggesting that here photosynthetic activity controls WUE_i rather than stomatal closure (Scheidegger et al., 2000). The increase of CWT in declining trees in ARG1 and the decrease in K_h would confirm this picture: here, trees could not grow or expand their tracheids, but they continued thickening their walls due to sufficient carbon availability, and increased their photosynthetic rates in response to drought. Moreover, these sites appeared as the mostly affected by the drought spell related to the 1998 drought. Following the conceptual model of Gessler et al. (2018) this action likely lead to hydraulic failure, finally triggering their dieback.

These different water-use strategies of *A. araucana* declining trees along a precipitation gradient from the coastal range near the Pacific Ocean to the Andes could be linked to microsite conditions (differences in altitudes and precipitation regime and amount). This would indicate that the relative roles played by mechanisms driving dieback are contingent on site conditions. Interestingly, different water use strategies were found in old-growth *Fitzroya cupressoides* stands located in the Coastal and the Andes range in Southern Chile (Urrutia-Jalabert et al., 2015). Similar to our results, *F. cupressoides* located at the coastal range presented lower growth with an increment of WUE_i (Arco Molina et al., 2019), whereas in the humid Andes range sites, it showed lower WUE_i denoting constant stomatal conductance under drought conditions, a potential cue of the

poor plastic adaptation of the species under rapid climate change (Camarero & Fajardo, 2017; Camarero et al., 2018; Urrutia-Jalabert et al., 2015). Similar results were also found in the *Erica arborea* in Italy since this Mediterranean shrub species, under different soil moisture, highlighted different WUE_i to cope with divergent water stress conditions (Battipaglia et al., 2014).

Recent studies across the Chilean Andes evidenced an increment in WUE_i and $\delta^{18}O$ in *Nothofagus pumilio* treelines, linked to reduce stomatal conductance, and associated to a reduction in growth (Fajardo et al., 2019; Lavergne et al., 2017). Likewise, long-term low growth and high WUE_i in declining trees was found in *P. sylvestris* in Switzerland, where the reduction in carbon availability triggered dieback (Timofeeva et al., 2017). Another hydraulic strategy to survive has been observed in declining *Pinus nigra* trees in Italy after extreme drought. There, declining trees produced larger tracheids (more vulnerable to cavitation), lower WUE_i (higher g_s), and high $\delta^{18}O$ (high transpiration rates) than nondeclining trees (Petrucco et al., 2017), a similar pattern to that observed in some *P. sylvestris* declining trees in Spain (Voltas et al., 2013). In addition, in southern Italy, the same pattern, with lower $\delta^{18}O$ values in nondeclining trees was observed in declining *Quercus frainetto* trees, and the authors considered hydraulic failure as the potential cause of dieback (Colangelo et al., 2017). Finally, the observed trends in tree-ring stables isotopes are seemingly associated to a twofold process: the common increase in WUE_i is likely related to the global plant responses to the increasing atmospheric CO_2 concentration (Walker et al., 2020), but here the improvement in WUE_i was more marked in declining trees from the drier sites indicating local, physiological responses. On the other side, the different responses in terms of $\delta^{13}C$ and $\delta^{18}O$ between declining and nondeclining trees across sites, with a stronger coupling in drier sites, together with the significant reduction in TRW and K_h started several decades before dieback symptoms such as leaf shedding were observed (Figure 4), might represent a common ground in the long-lasting deterioration of their hydraulic functioning as already observed (Gessler et al., 2018; Pellizzari et al., 2016). Despite the lack of common patterns, our study infers different site-contingent mechanisms of dieback and represents a new step forward for better understanding the xylem trait and physiological mechanisms that trigger drought induced dieback in temperate rainforests at long-term scales.

5 | CONCLUSIONS

This research confirms long-term retrospective quantifications of tree-ring growth, anatomical traits and tree-ring stable isotopes as relevant tools to forecast tree dieback. We proved this by comparing these variables in declining versus nondeclining *A. araucana* trees in Northern Patagonia. Dieback in this iconic South American conifer was triggered by the earlier deterioration in hydraulic functional traits, that leads to a reduce capacity of declining trees, with their lower K_h, to withstand extreme droughts respect to nondeclining trees. However, this pattern was not observed in all sites and depended on local climate conditions. Retrospective wood anatomical and isotope analyses provide multiproxy frameworks to identify and forecast which species, tree populations, and individuals will be more prone to drought-induced dieback, and which will be more resilient in response to warming and future drying trends. This information will be particularly valuable for the conservation of endangered tree species as *A. araucana*, one of the most emblematic tree of South American temperate rainforests. Nonetheless, this research raises many questions about the role of microsite topography and soil moisture conditions that could determine the differences in tree water use strategies to cope with drought and mechanisms leading to drought-induced dieback. Future research, considering a larger number of trees and sites, should also investigate if genetic variability (e.g., Bansal et al., 2015), sex (e.g. Hadad et al., 2021), or microsite features (e.g., soil depth) could contribute to better explain which individuals and populations are able to tolerate and adapt better under stressful water shortage.

ACKNOWLEDGMENTS

We are grateful to Cristián Frêne, Alejandro Martinez Meier, and Anne-Sophie Sergent for the support in the collection of *Araucaria araucana* samples. We thank Raffaella Dibona and Michele Colangelo for helping with measurements and analyses of wood microsections. We thank Claudia Puchi for the cell design in Figure 2. Paulina F. Puchi was also supported by The Rufford Foundation for Conservancy, project N°23677-1. We acknowledge Chilean Forest Service CONAF for permission N°851540 to collect the tree-ring samples in Altos de Pemehue National Reserve. We also thank the Argentinian National Parks Administration for permission to collect dendrochronological samples in Lanin National Park. Finally, we thank Forestal MININCO S.A. for the authorization to sample in Trongol Alto.

CONFLICT OF INTEREST

Paulina Puchi, during this research, was a PhD student under the supervision of Prof. M. Carrer at the TeSAF department of the University of Padova. They do not stand to gain or lose financially through this publication. The other authors declare no competing interests.

DATA AVAILABILITY STATEMENT

Data openly available in a public repository that issues datasets with DOIs.

ORCID

Paulina F. Puchi https://orcid.org/0000-0001-5429-8605
J. Julio Camarero https://orcid.org/0000-0003-2436-2922
Giovanna Battipaglia https://orcid.org/0000-0003-1741-3509
Marco Carrer https://orcid.org/0000-0003-1581-6259

REFERENCES

Adams, H. D., Zeppel, M. J. B., Anderegg, W. R. L., Hartmann, H., Landhäusser, S. M., Tissue, D. T., Huxman, T. E., Hudson, P. J.,

Franz, T. E., Allen, C. D., Anderegg, L. D. L., Barron-Gafford, G. A., Beerling, D. J., Breshears, D. D., Brodribb, T. J., Bugmann, H., Cobb, R. C., Collins, A. D., Dickman, L. T., … McDowell, N. G. (2017). A multi-species synthesis of physiological mechanisms in drought-induced tree mortality. *Nature Ecology and Evolution*, *1*, 1285–1291.

Aguilera-Betti, I., Muñoz, A. A., Stahle, D., Figueroa, G., Duarte, F., González-Reyes, Á., Christie, D., Lara, A., González, M. E., Sheppard, P. R., Sauchyn, D., Moreira-Muñoz, A., Toledo-Guerrero, A., Olea, M., Apaz, P., & Fernandez, A. (2017). The first millennium-age *Araucaria araucana* in Patagonia. *Tree-Ring Research*, *73*, 53–56.

Allen, C. D., Breshears, D. D., & McDowell, N. G. (2015). On underestimation of global vulnerability to tree mortality and forest die-off from hotter drought in the Anthropocene. *Ecosphere*, *6*, 1–55. https://doi.org/10.1890/ES15-00203.1

Allen, C. D., Macalady, A. K., Chenchouni, H., Bachelet, D., McDowell, N., Vennetier, M., Kitzberger, T., Rigling, A., Breshears, D. D., Hogg, E. H. (Ted), Gonzalez, P., Fensham, R., Zhang, Z., Castro, J., Demidova, N., Lim, J.-H., Allard, G., Running, S. W., Semerci, A., & Cobb, N. (2010). A global overview of drought and heat-induced tree mortality reveals emerging climate change risks for forests. *Forest Ecology and Management*, *259*, 660–684. https://doi.org/10.1016/j.foreco.2009.09.001

Amoroso, M. M., Daniels, L. D., & Larson, B. C. (2012). Temporal patterns of radial growth in declining *Austrocedrus chilensis* forests in Northern Patagonia: The use of tree-rings as an indicator of forest decline. *Forest Ecology and Management*, *265*, 62–70. https://doi.org/10.1016/j.foreco.2011.10.021

Anderegg, W. R. L., Kane, J. M., & Anderegg, L. D. L. (2013). Consequences of widespread tree mortality triggered by drought and temperature stress. *Nature Climate Change*, *3*, 30–36.

Arco Molina, J. G., Helle, G., Hadad, M. A., & Roig, F. A. (2019). Variations in the intrinsic water-use efficiency of North Patagonian forests under a present climate change scenario: Tree age, site conditions and long-term environmental effects. *Tree Physiology*, *39*, 661–678. https://doi.org/10.1093/treephys/tpy144

Bansal, S., Harrington, C. A., Gould, P. J., & St Clair, J. B. (2015). Climate-related genetic variation in drought-resistance of Douglas-fir (*Pseudotsuga menziesii*). *Global Change Biology*, *21*, 947–958. https://doi.org/10.1111/gcb.12719

Barbour, M. (2007). Stable oxygen isotope composition of plant tissue: A review. *Functional Plant Biology*, *34*, 83–94.

Battipaglia, G., De Micco, V., Brand, W. A., Linke, P., Aronne, G., Saurer, M., & Cherubini, P. (2010). Variations of vessel diameter and $\delta^{13}C$ in false rings of *Arbutus unedo* L. reflect different environmental conditions. *New Phytologist*, *188*, 1099–1112. https://doi.org/10.1111/j.1469-8137.2010.03443.x

Battipaglia, G., De Micco, V., Brand, W. A., Saurer, M., Aronne, G., Linke, P., & Cherubini, P. (2014). Drought impact on water use efficiency and intra-annual density fluctuations in *Erica arborea* on Elba (Italy). *Plant, Cell and Environment*, *37*, 382–391. https://doi.org/10.1111/pce.12160

Beguería, S., Vicente-Serrano, S. M., Reig, F., & Latorre, B. (2014). Standardized precipitation evapotranspiration index (SPEI) revisited: Parameter fitting, evapotranspiration models, tools, datasets and drought monitoring. *International Journal of Climatology*, *34*, 3001–3023. https://doi.org/10.1002/joc.3887

Belmecheri, S., & Lavergne, A. (2020). Compiled records of atmospheric CO_2 concentrations and stable carbon isotopes to reconstruct climate and derive plant ecophysiological indices from tree rings. *Dendrochronologia*, *63*, 125748.

Björklund, J., Fonti, M. V., Fonti, P., Van den Bulcke, J., & von Arx, G. (2021). Cell wall dimensions reign supreme: Cell wall composition is irrelevant for the temperature signal of latewood density/blue intensity in Scots pine. *Dendrochronologia*, *65*, 125785. https://doi.org/10.1016/j.dendro.2020.125785

Bréda, N., Huc, R., Granier, A., & Dreyer, E. (2006). Temperate forest trees and stands under severe drought: A review of ecophysiological responses, adaptation processes and long-term consequences. *Annals of Forest Science*, *63*, 625–644. https://doi.org/10.1051/forest:2006042

Brodribb, T. J., Holbrook, N. M., Zwieniecki, M. A., & Palma, B. (2004). Leaf hydraulic capacity in ferns, conifers and angiosperms: Impacts on photosynthetic maxima. *New Phytologist*, *165*, 839–846. https://doi.org/10.1111/j.1469-8137.2004.01259.x

Brodribb, T. J., Powers, J., Cochard, H., & Choat, B. (2020). Hanging by a thread? Forests and drought. *Science*, *368*(6488), 261–266. https://doi.org/10.1126/science.aat7631

Bunn, A. G. (2008). A dendrochronology program library in R (dplR). *Dendrochronologia*, *26*, 115–124. https://doi.org/10.1016/j.dendro.2008.01.002

Bunn, A., Korpela, M., Biondi, F., Campelo, F., Mérian, P., Qeadan, F., & Zang, C. (2021). dplR: Dendrochronology program library in R. https://CRAN.R-project.org/package=dplR

Cailleret, M., Dakos, V., Jansen, S., Robert, E. M. R., Aakala, T., Amoroso, M. M., Antos, J. A., Bigler, C., Bugmann, H., Caccianaga, M., Camarero, J.-J., Cherubini, P., Coyea, M. R., Čufar, K., Das, A. J., Davi, H., Gea-Izquierdo, G., Gillner, S., Haavik, L. J., … Martínez-Vilalta, J. (2019). Early-warning signals of individual tree mortality based on annual radial growth. *Frontiers in Plant Science*, *9*, 1964. https://doi.org/10.3389/fpls.2018.01964

Cailleret, M., Jansen, S., Robert, E. M. R., Desoto, L., Aakala, T., Antos, J. A., Beikircher, B., Bigler, C., Bugmann, H., Caccianiga, M., Čada, V., Camarero, J. J., Cherubini, P., Cochard, H., Coyea, M. R., Čufar, K., Das, A. J., Davi, H., Delzon, S., … Martínez-Vilalta, J. (2016). A synthesis of radial growth patterns preceding tree mortality. *Global Change Biology*, *23*, 1675–1690. https://doi.org/10.1111/gcb.13535

Camarero, J. J., & Fajardo, A. (2017). Poor acclimation to current drier climate of the long-lived tree species Fitzroya cupressoides in the temperate rainforest of southern Chile. *Agricultural and Forest Meteorology*, *239*, 141–150.

Camarero, J. J., Gazol, A., Sangüesa-Barreda, G., & Fajardo, A. (2018). Coupled climate–forest growth shifts in the Chilean Patagonia are decoupled from trends in water–use efficiency. *Agricultural and Forest Meteorology*, *259*, 222–231. https://doi.org/10.1016/j.agrformet.2018.04.024

Camarero, J. J., Gazol, A., Sangüesa-Barreda, G., Oliva, J., & Vicente-Serrano, S. M. (2015). To die or not to die: Early warnings of tree dieback in response to a severe drought. *Journal of Ecology*, *103*, 44–57. https://doi.org/10.1111/1365-2745.12295

Carrer, M., Unterholzner, L., & Castagneri, D. (2018). Wood anatomical traits highlight complex temperature influence on *Pinus cembra* at high elevation in the Eastern Alps. *International Journal of Biometeorology*, *62*, 1745–1753. https://doi.org/10.1007/s00484-018-1577-4

Carrer, M., von Arx, G., Castagneri, D., & Petit, G. (2015). Distilling allometric and environmental information from time series of conduit size: The standardization issue and its relationship to tree hydraulic architecture. *Tree Physiology*, *35*, 27–33. https://doi.org/10.1093/treephys/tpu108

Castagneri, D., Battipaglia, G., Von Arx, G., Pacheco, A., & Carrer, M. (2018). Tree-ring anatomy and carbon isotope ratio show both direct and legacy effects of climate on bimodal xylem formation in *Pinus pinea*. *Tree Physiology*, *38*, 1098–1109. https://doi.org/10.1093/treephys/tpy036

Castagneri, D., Fonti, P., Arx, G. V., & Carrer, M. (2017). How does climate influence xylem morphogenesis over the growing season ? Insights from long-term intra-ring anatomy in *Picea abies*. *Annals of Botany*, *119*, 1011–1020. https://doi.org/10.1093/aob/mcw274

Center for Information of Natural Resources - CIREN. (2010). *Determination of the current and potential soil erosion risk in Chile* (p. 145). CIREN.

Cherubini, P., Battipaglia, G., & Innes, J. (2021). Tree vitality and forest health: Can tree-ring stable isotopes be used as indicators? *Current Forestry Reports*, *7*(2), 69–80. https://doi.org/10.1007/s40725-021-00137-8

Colangelo, M., Camarero, J. J., Battipaglia, G., Borghetti, M., De Micco, V., Gentilesca, T., & Ripullone, F. (2017). A multi-proxy assessment of dieback causes in a Mediterranean oak species. *Tree Physiology*, *37*, 617–631. https://doi.org/10.1093/treephys/tpx002

Cook, E. R., & Kairiukstis, L. A. (Eds.). (1990). *Methods of dendrochronology: Applications in the environmental sciences*. IIASA-Kluwer.

Cuny, H. E., Fonti, P., Rathgeber, C. B. K., von Arx, G., Peters, R. L., & Frank, D. C. (2018). Couplings in cell differentiation kinetics mitigate air temperature influence on conifer wood anatomy. *Plant Cell and Environment*, *42*(4), 1222–1232. https://doi.org/10.1111/pce.13464

Cuny, H. E., Rathgeber, C. B. K., Frank, D., Fonti, P., Mäkinen, H., Prislan, P., Rossi, S., del Castillo, E. M., Campelo, F., Vavrčík, H., Camarero, J. J., Bryukhanova, M. V., Jyske, T., Gričar, J., Gryc, V., De Luis, M., Vieira, J., Čufar, K., Kirdyanov, A. V., … Fournier, M. (2015). Woody biomass production lags stem-girth increase by over one month in coniferous forests. *Nature Plants*, *15160*, 1–6. https://doi.org/10.1038/NPLANTS.2015.160

Dawson, T. E., Mambelli, S., Plamboeck, A. H., Templer, P. H., & Tu, K. P. (2002). Stable isotopes in plant ecology. *Annual Review of Ecology and Systematics*, *33*, 507–559. https://doi.org/10.1146/annurev.ecolsys.33.020602.095451

Drake, P. L., & Franks, P. J. (2003). Water resource partitioning, stem xylem hydraulic properties, and plant water use strategies in a seasonally dry riparian tropical rainforest. *Oecologia*, *137*, 321–329. https://doi.org/10.1007/s00442-003-1352-y

Ehleringer, J. R., Hall, A. E., & Farquhar, G. D. (1993). *Stable isotopes and plant carbon/water relations*. Academic Press.

Fajardo, A., Gazol, A., Mayr, C., & Camarero, J. J. (2019). Recent decadal drought reverts warming-triggered growth enhancement in contrasting climates in the southern Andes tree line. *Journal of Biogeography*, *46*, 1367–1379. https://doi.org/10.1111/jbi.13580

Farquhar, G. D., O'Leary, M. H., & Berry, J. A. (1982). On the relationship between carbon isotope discrimination and the intercellular carbon dioxide concentration in leaves. *Australian Journal of Plant Physiology*, *9*, 121–137.

Farquhar, G. D., & Richards, R. A. (1984). Isotopic composition of plant carbon correlates with water-use efficiency of wheat genotypes. *Australian Journal of Plant Physiology*, *11*, 539–552.

Fonti, P., Von Arx, G., García-González, I., Eilmann, B., Sass-Klaassen, U., Gärtner, H., & Eckstein, D. (2010). Studying global change through investigation of the plastic responses of xylem anatomy in tree rings. *New Phytologist*, *185*, 42–53. https://doi.org/10.1111/j.1469-8137.2009.03030.x

Francey, R. J., Allison, C. E., Etheridge, D. M., Trundinger, C. M., Enting, I. G., Leuenberger, M., Langenfelds, R. L., Michel, E., & Steele, L. P. (1999). A 1000- year high precision record of $\delta^{13}C$ in atmospheric CO_2. *Tellus B: Chemical and Physical Meteorology*, *51*(2), 170–193. https://doi.org/10.3402/tellusb.v51i2.16269

Garreaud, R. D., Boisier, J. P., Rondanelli, R., Montecinos, A., Sepúlveda, H. H., & Veloso-Aguila, D. (2019). The Central Chile Mega Drought (2010–2018): A climate dynamics perspective. *International Journal of Climatology*, *40*, 421–439. https://doi.org/10.1002/joc.6219

Gessler, A., Cailleret, M., Joseph, J., Schönbeck, L., Schaub, M., Lehmann, M., Treydte, K., Rigling, A., Timofeeva, G., & Saurer, M. (2018). Drought induced tree mortality – A tree-ring isotope based conceptual model to assess mechanisms and predispositions. *New Phytologist*, *219*, 485–490. https://doi.org/10.1111/nph.15154

Hadad, M. A., Roig, F. A., Arco Molina, J. G., & Hacket-Pain, A. (2021). Growth of male and female *Araucaria araucana* trees respond differently to regional mast events, creating sex-specific patterns in their tree-ring chronologies. *Ecological Indicators*, *122*, 107245. https://doi.org/10.1016/j.ecolind.2020.107245

Hammond, W. M., Yu, K., Wilson, L. A., Will, R. E., Anderegg, W. R. L., & Adams, H. D. (2019). Dead or dying? Quantifying the point of no return from hydraulic failure in drought-induced tree mortality. *New Phytologist*, *223*, 1834–1843. https://doi.org/10.1111/nph.15922

Hentschel, R., Rosner, S., Kayler, Z. E., Andreassen, K., Børja, I., Solberg, S., Tveito, O. E., Priesack, E., & Gessler, A. (2014). Norway spruce physiological and anatomical predisposition to dieback. *Forest Ecology and Management*, *322*, 27–36. https://doi.org/10.1016/j.foreco.2014.03.007

Holmes, R. L. (1983). Computer-assisted quality control in tree-ring dating and measurement. *Tree-Ring Bulletin*, *43*, 69–78.

Jia, G., Shevliakova, E., Artaxo, P., De Noblet-Ducoudré, N., Houghton, R., House, J., Kitajima, K., Lennard, C., Popp, A., Sirin, A., Sukumar, R., & Verchot, L. (2019). Land–climate interactions. In P. R. Shukla, J. Skea, E. Calvo Buendia, V. Masson-Delmotte, H.-O. Pörtner, D. C. Roberts, P. Zhai, R. Slade, S. Connors, R. van Diemen, M. Ferrat, E. Haughey, S. Luz, S. Neogi, M. Pathak, J. Petzold, J. Portugal Pereira, P. Vyas, E. Huntley, … J. Malley (Eds.), *Climate Change and Land: An IPCC special report on climate change, desertification, land degradation, sustainable land management, food security, and greenhouse gas fluxes in terrestrial ecosystems* (pp. 1–186). WMO.

Jolliffe, I. T. (2002). *Principal component analysis*. Springer.

Kagawa, A., Sugimoto, A., & Maximov, T. C. (2006). $^{13}CO_2$ pulse-labelling of photoassimilates reveals carbon allocation within and between tree rings. *Plant, Cell and Environment*, *29*, 1571–1584. https://doi.org/10.1111/j.1365-3040.2006.01533.x

Kitzberger, T., Swetnam, T. W., & Veblen, T. T. (2001). Inter-hemispheric synchrony of forest fires and the El Niño-Southern Oscillation. *Global Ecology and Biogeography*, *10*, 315–326. https://doi.org/10.1046/J.1466-822X.2001.00234.X

Kuptz, D., Fleischmann, F., Matyssek, R., & Grams, T. (2011). Seasonal patterns of carbon allocation to respiratory pools in 60-yr-old deciduous (*Fagus sylvatica*) and evergreen (*Picea abies*) trees assessed via whole-tree stable carbon isotope labeling. *New Phytologist*, *191*, 160–172. https://doi.org/10.1111/j.1469-8137.2011.03676.x

Lavergne, A., Daux, V., Villalba, R., Pierre, M., Stievenard, M., & Srur, A. M. (2017). Improvement of isotope-based climate reconstructions in Patagonia through a better understanding of climate influences on isotopic fractionation in tree rings. *Earth and Planetary Science Letters*, *459*, 372–380. https://doi.org/10.1016/j.epsl.2016.11.045

Liang, W., Heinrich, I., Simard, S., Helle, G., Liñán, I. D., & Heinken, T. (2013). Climate signals derived from cell anatomy of scots pine in NE Germany. *Tree Physiology*, *33*(8), 833–844. https://doi.org/10.1093/treephys/tpt059

McDowell, N. G., Allen, C. D., Anderson-Teixeira, K., Aukema, B. H., Bond-Lamberty, B., Chini, L., Clark, J. S., Dietze, M., Grossiord, C., Hanbury-Brown, A., Hurtt, G. C., Jackson, R. B., Johnson, D. J., Kueppers, L., Lichstein, J. W., Ogle, K., Poulter, B., Pugh, T. A. M., Seidl, R., … Xu, C. (2020). Pervasive shifts in forest dynamics in a changing world. *Science*, *368*, eaaz9463. https://doi.org/10.1126/science.aaz9463

McDowell, N., Pockman, W. T., Allen, C. D., Breshears, D. D., Cobb, N., Kolb, T., Plaut, J., Sperry, J., West, A., Williams, D. G., & Yepez, E. A. (2008). Mechanisms of plant survival and mortality during drought: Why do some plants survive while others succumb to drought? *New Phytologist*, *178*, 719–739. https://doi.org/10.1111/j.1469-8137.2008.02436.x

Miranda, A., Lara, A., Altamirano, A., Di Bella, C., González, M. E., & Camarero, J. (2020). Forest browning trends in response to drought in a highly threatened mediterranean landscape of South America. *Ecological Indicators*, *115*, 106401. https://doi.org/10.1016/j.ecolind.2020.106401

Moreno-Gutiérrez, C., Dawson, T. E., Nicolás, E., & Querejeta, J. I. (2012). Isotopes reveal contrasting water use strategies among coexisting plant species in a Mediterranean ecosystem. *New Phytologist*, *196*, 489–496. https://doi.org/10.1111/j.1469-8137.2012.04276.x

Muñoz, A. A., González-Reyes, A., Lara, A., Sauchyn, D., Christie, D., Puchi, P., Urrutia-Jalabert, R., Toledo-Guerrero, I., Aguilera-Betti, I., Mundo, I., Sheppard, P. R., Stahle, D., Villalba, R., Szejner, P., LeQuesne, C., & Vanstone, J. (2016). Streamflow variability in the Chilean Temperate-Mediterranean climate transition (35°S–42°S) during the last 400 years inferred from tree-ring records. *Climate Dynamics*, *47*, 4051–4066. https://doi.org/10.1007/s00382-016-3068-9

Norton, D. A., Palmer, J. G., & Ogden, J. (1987). Dendroecological studies in New Zealand 1. An evaluation of tree age estimates based on increment cores. *New Zealand Journal of Botany*, *25*, 373–383.

Pacheco, A., Camarero, J. J., Pompa-García, M., Battipaglia, G., Voltas, J., & Carrer, M. (2020). Growth, wood anatomy and stable isotopes show species-specific couplings in three Mexican conifers inhabiting drought-prone areas. *Science of the Total Environment*, *698*, 134055. https://doi.org/10.1016/j.scitotenv.2019.134055

Pellizzari, E., Camarero, J. J., Gazol, A., Sangüesa-Barreda, G., & Carrer, M. (2016). Wood anatomy and carbon-isotope discrimination support long-term hydraulic deterioration as a major cause of drought-induced dieback. *Global Change Biology*, *22*, 2125–2137. https://doi.org/10.1111/gcb.13227

Peres-Neto, P. R., Jackson, D. A., & Somers, K. M. (2005). How many principal components? Stopping rules for determining the number of non-trivial axes revisited. *Computational Statistics & Data Analysis*, *49*, 974–997. https://doi.org/10.1016/j.csda.2004.06.015

Petrucco, L., Nardini, A., Von Arx, G., Saurer, M., & Cherubini, P. (2017). Isotope signals and anatomical features in tree rings suggest a role for hydraulic strategies in diffuse drought-induced die-back of *Pinus nigra*. *Tree Physiology*, *37*, 523–535. https://doi.org/10.1093/treephys/tpx031

Premoli, A., Quiroga, P., & Gardner, M. (2013). *Araucaria araucana*. The IUCN red list of threatened species 2013: e.T31355A2805113. https://doi.org/10.2305/IUCN.UK.2013-1.RLTS.T31355A2805113.en. Downloaded on 20 October 2020.

Prendin, A. L., Petit, G., Carrer, M., Fonti, P., Björklund, J., & von Arx, G. (2017). New research perspectives from a novel approach to quantify tracheid wall thickness. *Tree Physiology*, *37*(7), 976–983. https://doi.org/10.1093/treephys/tpx037

Puchi, P. F., Castagneri, D., Rossi, S., & Carrer, M. (2019). Wood anatomical traits in black spruce reveal latent water constraints on the boreal forest. *Global Change Biology*, *26*(3), 1767–1777. https://doi.org/10.1111/gcb.14906

R Core Team. (2021). *R: A language and environment for statistical computing*. R Foundation for Statistical Computing.

Ripullone, F., Camarero, J. J., Colangelo, M., & Voltas, J. (2020). Variation in the access to deep soil water pools explains tree-to-tree differences in drought-triggered dieback of Mediterranean oaks. *Tree Physiology*, *40*, 591–604. https://doi.org/10.1093/treephys/tpaa026

Saurer, M., Siegwolf, R. T. W., & Schweingruber, F. H. (2004). Carbon isotope discrimination indicates improving water-use efficiency of trees in northern Eurasia over the last 100 years. *Global Change Biology*, *10*, 2109–2120. https://doi.org/10.1111/j.1365-2486.2004.00869.x

Scheidegger, Y., Saurer, M., Bahn, M., & Siegwolf, R. (2000). Linking stable oxygen and carbon isotopes with stomatal conductance and photosynthetic capacity: A conceptual model. *Oecologia*, *125*, 350–357. https://doi.org/10.1007/s004420000466

Schulman, E. (1956). *Dendroclimatic change in semiarid America*. University of Arizona Press.

Seibt, U., Rajabi, A., Griffiths, H., & Berry, J. (2008). Carbon isotopes and water use efficiency: Sense and sensitivity. *Oecologia*, *155*, 441–454. https://doi.org/10.1007/s00442-007-0932-7

Serrano-León, H., & Christie, D. A. (2020). Tree-growth at the rear edge of a *Nothofagus pumilio* Andean forest from Northern Patagonia show different patterns and a decline in the common signal during the last century. *Forest Ecology and Management*, *475*, 118426. https://doi.org/10.1016/j.foreco.2020.118426

Soudant, A., Loader, N. J., Bäck, J., Levula, J., & Kljun, N. (2016). Intra-annual variability of wood formation and δ 13C in tree-rings at Hyytiälä, Finland. *Agricultural & Forest Meteorology*, *224*, 17–29. https://doi.org/10.1016/j.agrformet.2016.04.015

Stokes, M. A., & Smiley, T. L. (1968). *An introduction to tree-ring dating*. The University of Chicago Press.

Suarez, M. L., Ghermandi, L., & Kitzberger, T. (2004). Factors predisposing episodic drought induced tree mortality in Nothofagus–site, climatic sensitivity and growth trends. *Journal of Ecology*, *92*, 954–966. https://doi.org/10.1111/j.1365-2745.2004.00941.x

Timofeeva, G., Treydte, K., Bugmann, H., Rigling, A., Schaub, M., Siegwolf, R., & Saurer, M. (2017). Long-term effects of drought on tree-ring growth and carbon isotope variability in Scots pine in a dry environment. *Tree Physiology*, *37*, 1028–1041. https://doi.org/10.1093/treephys/tpx041

Trenberth, K. E., Dai, A., van der Schrier, G., Jones, P. D., Barichivich, J., Briffa, K. R., & Sheffield, J. (2014). Global warming and changes in drought. *Nature Climate Change*, *4*, 17–22. https://doi.org/10.1038/nclimate2067

Trugman, A. T., Anderegg, L. D. L., Anderegg, W. R. L., Das, A. J., & Stephenson, N. L. (2021). Why is tree drought mortality so hard to predict? *Trends in Ecology and Evolution*, *36*(6), 520–532. https://doi.org/10.1016/j.tree.2021.02.001

Urrutia-Jalabert, R., Malhi, Y., Barichivich, J., Lara, A., Delgado-Huertas, A., Rodríguez, C. G., & Cuq, E. (2015). Increased water use efficiency but contrasting tree growth patterns in *Fitzroya cupressoides* forests of southern Chile during recent decades. *Journal of Geophysical Research: Biogeosciences*, *120*, 2505–2524. https://doi.org/10.1002/2015JG003098

Veblen, T. T., Burns, B. R., Kitzberger, T., Lara, A., & Villalba, A. (1995). The ecology of the conifers of southern South America. In N. J. Enright & R. S. Hill (Eds.), *Ecology of the Southern Conifers* (pp. 129–135). Melbourne University Press.

Vicente-Serrano, S. M., Beguería, S., & López-Moreno, J. I. (2010). A Multiscalar drought index sensitive to global warming: The Standardized Precipitation Evapotranspiration Index - SPEI. *Journal of Climate*, *23*, 1696–1718. https://doi.org/10.1175/2009JCLI2909.1

Villalba, R., Lara, A., Masiokas, M. H., Urrutia, R., Luckman, B. H., Marshall, G. J., Mundo, I. A., Christie, D. A., Cook, E. R., Neukom, R., Allen, K., Fenwick, P., Boninsegna, J. A., Srur, A. M., Morales, M. S., Araneo, D., Palmer, J. G., Cuq, E., Aravena, J. C., … LeQuesne, C. (2012). Unusual Southern Hemisphere tree growth patterns induced by changes in the Southern Annular Mode. *Nature Geoscience*, *5*(11), 793–798. https://doi.org/10.1038/ngeo1613

Villalba, R., & Veblen, T. T. (1998). Influences of large-scale climatic variability on episodic tree mortality in northern Patagonia. *Ecology*, *79*, 2624–2640.

Voltas, J., Camarero, J. J., Carulla, D., Aguilera, M., Oriz, A., & Ferrio, J. P. (2013). A retrospective, dual-isotope approach reveals individual predispositions to winter-drought induced tree dieback in the southernmost distribution limit of Scots pine. *Plant, Cell and Environment*, *36*, 1435–1448. https://doi.org/10.1111/pce.12072

von Arx, G., Arzac, A., Fonti, P., Frank, D., Zweifel, R., Rigling, A., Galiano, L., Gessler, A., & Olano, J. M. (2017). Responses of sapwood ray parenchyma and non-structural carbohydrates of *Pinus sylvestris* to drought and long-term irrigation. *Functional Ecology*, *31*(7), 1371–1382. https://doi.org/10.1111/1365-2435.12860

von Arx, G., & Carrer, M. (2014). Roxas -A new tool to build centuries-long tracheid-lumen chronologies in conifers. *Dendrochronologia*, *32*(3), 290–293. https://doi.org/10.1016/j.dendro.2013.12.001

von Arx, G., Crivellaro, A., Prendin, A. L., Čufar, K., & Carrer, M. (2016). Quantitative wood anatomy—practical guidelines. *Frontiers in Plant Science*, *7*, 781. https://doi.org/10.3389/fpls.2016.00781

Walker, A. P., De Kauwe, M. G., Bastos, A., Belmecheri, S., Georgiou, K., Keeling, R. F., & Zuidema, P. A. (2020). Integrating the evidence for a terrestrial carbon sink caused by increasing atmospheric CO_2. *New Phytologist*, https://doi.org/10.1111/nph.16866

Zimmer, H. C., Brodribb, T. J., Delzon, S., & Baker, P. J. (2015). Drought avoidance and vulnerability in the Australian Araucariaceae. *Tree Physiology*, *36*(2), 218–228. https://doi.org/10.1093/treephys/tpv111

Zweifel, R., Zimmermann, L., Zeugin, F., & Newbery, D. M. (2006). Intra-annual radial growth and water relations of trees: Implications towards a growth mechanism. *Journal of Experimental Botany*, *57*, 1445–1459.

SUPPORTING INFORMATION

Additional supporting information may be found in the online version of the article at the publisher's website.

How to cite this article: Puchi PF, Camarero JJ, Battipaglia G, Carrer M. Retrospective analysis of wood anatomical traits and tree-ring isotopes suggests site-specific mechanisms triggering *Araucaria araucana* drought-induced dieback. *Glob Change Biol*. 2021;27:6394–6408. https://doi.org/10.1111/gcb.15881